
PICTORIAL ESSAY

Post-irradiation Changes and Complications of Nasopharyngeal Carcinoma: A Review of Imaging Features

JCY Lau, JHM Cheng, SY Luk, JLS Khoo

Department of Radiology, Pamela Youde Nethersole Eastern Hospital, Chai Wan, Hong Kong

INTRODUCTION

Nasopharyngeal carcinoma (NPC) is a relatively common malignancy in Hong Kong. Radiotherapy (RT) plays a major role in the treatment of early and intermediate stage disease. Despite advancement from conventional two-dimensional RT to three-dimensional or intensity-modulated RT, post-irradiation changes and complications are still commonly encountered. These changes may evolve over time and may manifest early or years after completion of RT. Differentiating these expected post-irradiation changes from residual tumour and disease recurrence can be challenging.

This article aims to review the imaging features of common post-irradiation changes at different stages of treatment and a broad spectrum of irradiation-related complications in patients with NPC.

COMMON POST-IRRADIATION CHANGES

Mucocutaneous Changes

Mucocutaneous tissue is commonly affected by radiation due to its high radiosensitivity, causing mucositis. Inflammation can be due to direct irradiation and/or increased epithelial susceptibility to infection. Diagnosis is based mainly on clinical findings, although pharyngeal

mucosal hyperenhancement and thickening can be encountered radiologically at the early stage (Figure 1).

Chronic mucositis can appear as mucosal atrophy, necrosis and/or ulcerative changes, posing difficulty in distinguishing them from malignant changes.¹ Other chronic changes including choanal atresia, paranasal sinus mucocele, and polyp formation have also been reported.²

Glandular Changes

One of the most common potentially highly disabling side-effects of RT in the head and neck region is xerostomia.² The salivary glands are frequently affected by radiation, transiently or permanently. Glandular tissue may appear oedematous (Figure 2) with heterogeneous signal and enhancement on magnetic resonance imaging (MRI) at the early treatment stage. Atrophy and/or fatty infiltration may be encountered at a later stage of treatment (Figure 3).³

The pituitary gland may also be damaged by irradiation, impairing the hypothalamic-pituitary hormonal axis with consequent hormonal deficiencies. Nonetheless MRI findings are usually unremarkable despite the presence of symptomatic neuroendocrine deficiency.²

Correspondence: Dr JCY Lau, Department of Radiology, Pamela Youde Nethersole Eastern Hospital, Chai Wan, Hong Kong
Email: jackylcy135@yahoo.com.hk

Submitted: 26 Mar 2019; Accepted: 3 Jun 2019.

Contributors: JHMC, SYL and JLSK designed the study; JCYL and JHMC acquired and analysed the data; JCYL drafted the manuscript; JHMC, SYL and JLSK critically revised the manuscript for important intellectual content. All authors had full access to the data, contributed to the study, approved the final version for publication, and take responsibility for its accuracy and integrity.

Conflicts of Interest: The authors have no conflict of interest to declare.

Funding/Support: This pictorial essay received no specific grant from any funding agency in the public, commercial, or not-for-profit sectors.

Ethics Approval: This study was approved by the Hospital Authority Hong Kong East Cluster Research Ethics Committee (Ref HKECREC-2019-037).

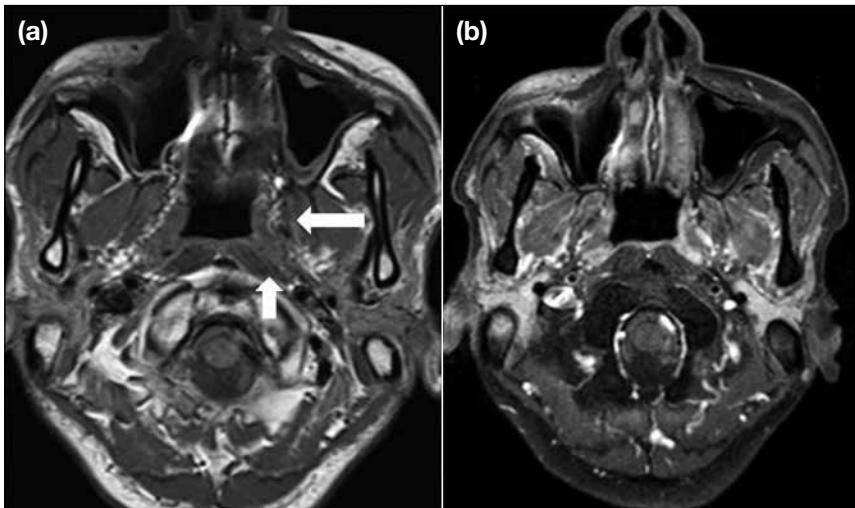


Figure 1. Magnetic resonance imaging in axial (a) T1-weighted and (b) post-gadolinium with fat saturation sequences. Asymmetrical mucosal thickening with mild enhancement is seen at the left nasopharynx (arrows) in a patient who recently completed radiotherapy. Clinical and endoscopic examinations showed no evidence of recurrence.

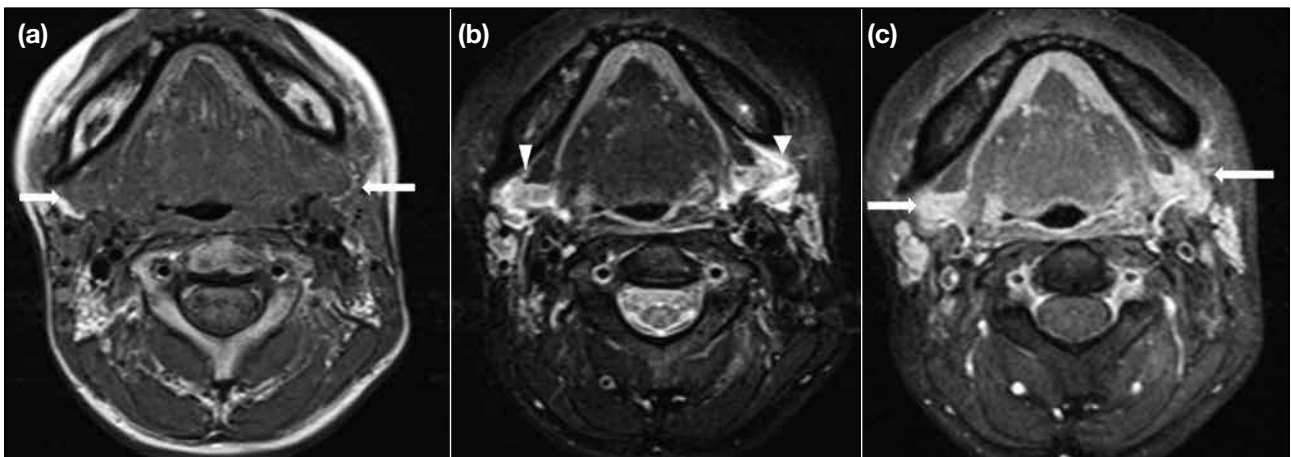


Figure 2. Magnetic resonance imaging of bilateral submandibular glands in axial (a) T1-weighted, (b) T2-weighted, and (c) post-gadolinium with fat saturation sequences. T2 hyperintense signals (arrowheads) with mild contrast enhancement (arrows) were evident in both submandibular glands, compatible with sialadenitis.

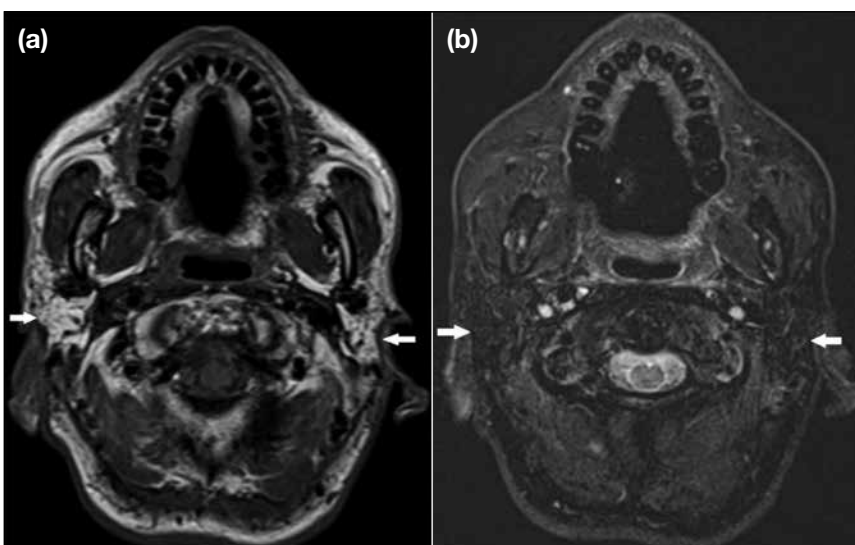


Figure 3. Axial magnetic resonance imaging (a) T1-weighted and (b) T2-weighted fat saturation sequences showing fatty atrophy of bilateral parotid glands (arrows), compatible with chronic sialadenitis.

Sinusitis and Otomastoiditis

Post-irradiation and at the early stage of treatment, patients commonly experience a certain degree of sinusitis and/or otomastoiditis (Figure 4), mainly due to reactive oedema of the mucosa and blockage of meatal openings. The incidence of mastoiditis usually increases during the first few months of treatment. Imaging features include T2-weighted (TW2) hyperintense effusion, with or without contrast enhancement and restricted diffusion. In severe cases, subperiosteal abscess may develop.⁴

Over time, chronic sinusitis and/or otomastoiditis are observed in some irradiated patients, although the incidence is lower than during early treatment.⁴ The acute inflammation may become crusted with adhesions months to years after completion of RT.

Radiation-induced osteitis

Radiation-induced osteitis is commonly asymptomatic and involves the sphenoid bone at the skull base and upper cervical spine. Radiation-induced fatty replacement

of marrow is the most common osseous imaging abnormality in post-irradiation patients, although initial imaging may be normal. On computed tomography, a mottled appearance of the skull base with mixed patchy sclerosis and lucency and coarsened trabeculum can be observed (Figure 5).¹ Further progression to osteoradionecrosis with osseous changes can be seen in some cases and will be further discussed later on.

Others

Other common changes including trismus, skin and neck fibrosis are beyond the scope of this review.

POST-RADIATION COMPLICATIONS

Radiation Injury to the Nervous System

Temporal Lobe Necrosis

One of the most debilitating and serious neurological complications is temporal lobe necrosis (TLN). It has a latent period of 1.5 to 13 years.⁵ The inferomedial aspects of the temporal lobes are most commonly involved due to their close proximity to the radiation field at the skull base, with bilateral involvement in up to approximately two-thirds of patients.⁶ Histological examination shows oedema, reactive gliosis and demyelination, followed by

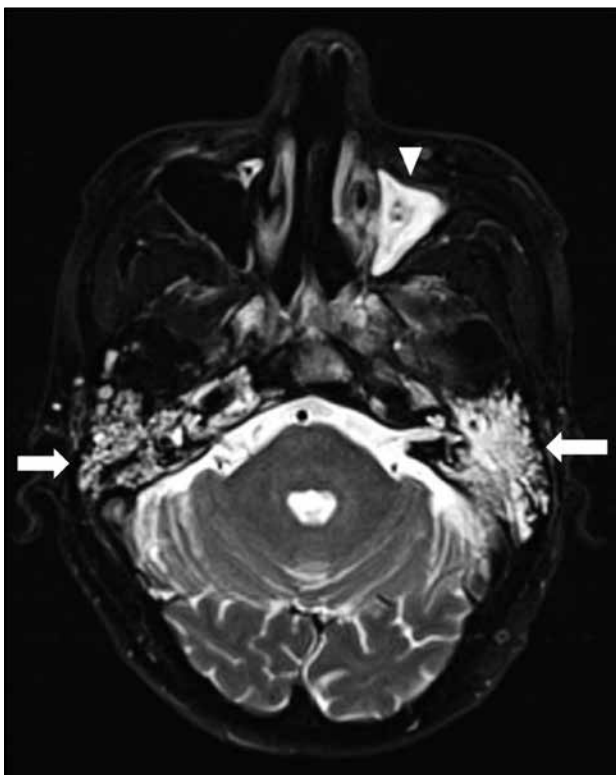


Figure 4. Magnetic resonance imaging in axial T2-weighted sequence showing mucosal thickening at the left maxillary sinus, representing sinusitis changes (arrowhead). T2-weighted hyperintensity at both mastoid air cells represents mastoid effusion (arrows).

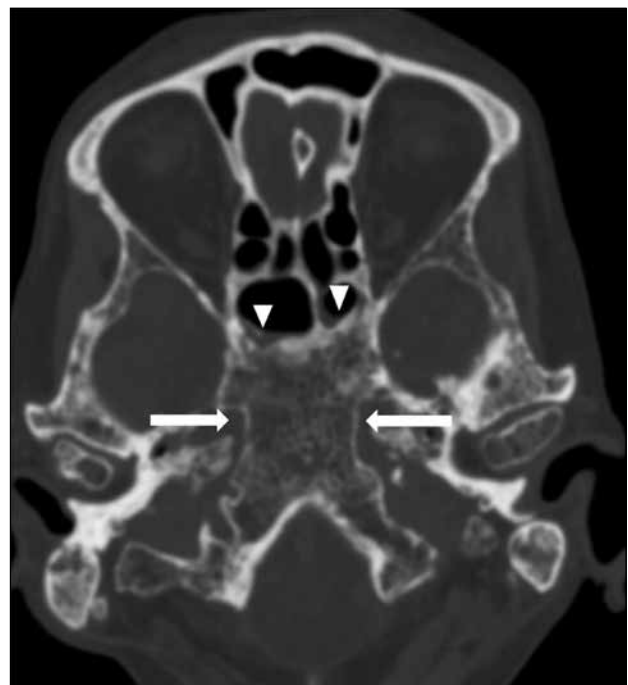


Figure 5. Axial computed tomography in bone window showing patchy sclerotic and lytic changes at the skull base, representing radiation-induced osteitis (arrows). Mucosal thickening is seen at both sphenoid sinuses, representing sinusitis (arrowheads).

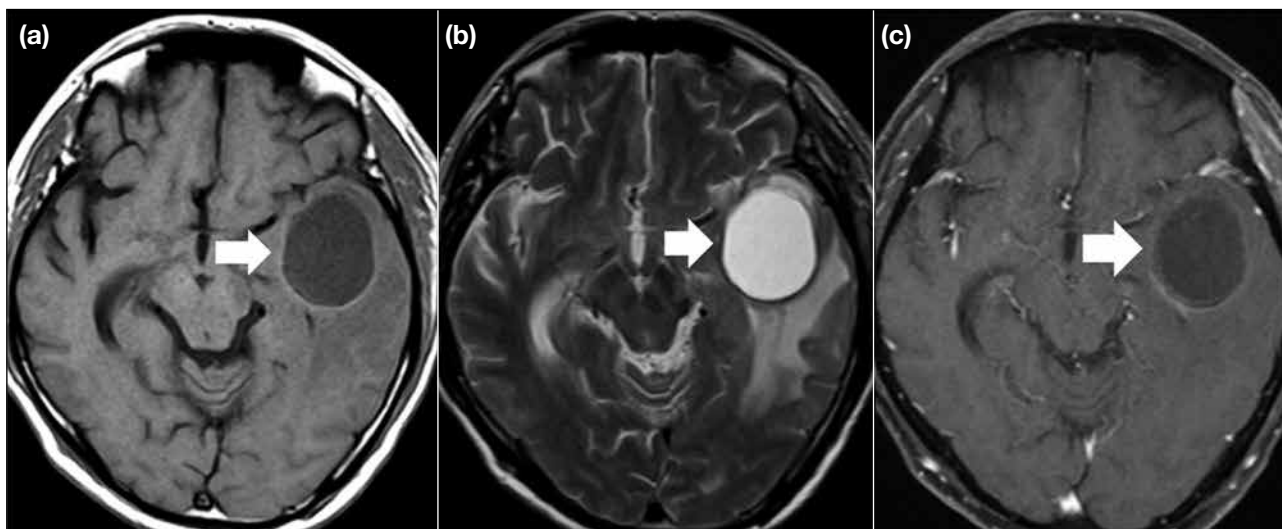


Figure 6. Magnetic resonance imaging axial images in (a) T1-weighted, (b) T2-weighted, and (c) T1-weighted post-gadolinium with fat saturation sequences, showing a cystic lesion at the left temporal lobe with mass effect (arrows) and background temporal lobe necrosis. Surgical drainage and excision were performed with histology confirming radionecrosis.

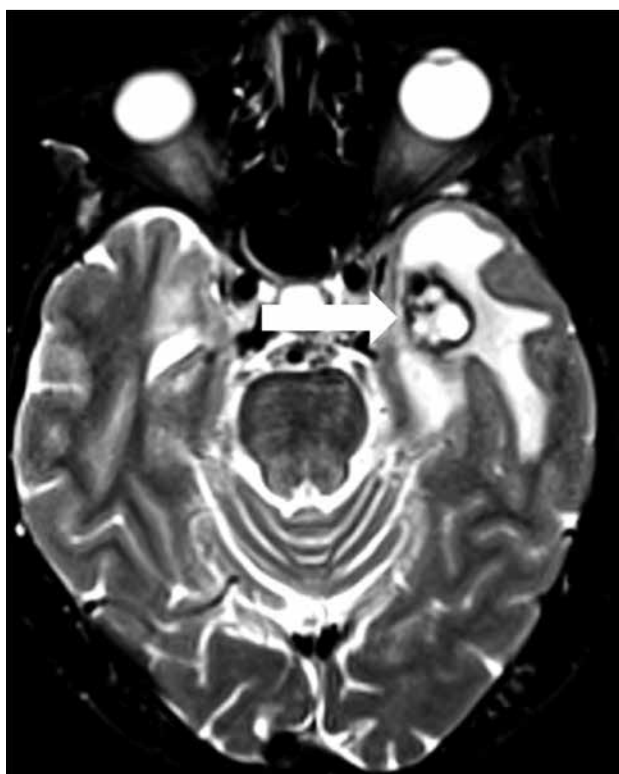


Figure 7. Magnetic resonance imaging axial T2-weighted sequence reveals asymmetrical T2-weighted hyperintense signal over bilateral temporal lobes, suggestive of temporal lobe necrosis. A heterogenous lobulated T2-weighted hyperintense lesion with hypointense rim (arrow) is seen over the medial left temporal lobe, compatible with previous haemorrhage.

cavitation and necrosis. Imaging findings include focal or extensive homogenous T2W hyperintensity in the white matter, representing white matter rarefaction of myelin or oedema. Associated mass effect may be present, especially when there is extensive white matter injury. Grey matter lesions occur in up to 90% of patients but are usually less extensive,⁷ with the inferior aspects of the temporal lobes being most susceptible since they receive a higher radiation dosage. MRI shows necrotic foci and contrast enhancing lesions that may progress or resolve over time.² In some cases, TLN may be complicated by cystic formation (Figure 6) or haemorrhage at later stages (Figure 7).⁸ Steroid is thought to be useful to reduce the oedema of TLN.⁷

Cranial Nerve Palsy

The second most common site of neurological injury is the cranial nerves, especially the hypoglossal nerve, followed by the vagus nerve and recurrent laryngeal nerve.⁹ MRI may demonstrate secondary signs of cranial nerve palsy that include oedema, fatty infiltration and atrophy of the respective muscles supplied by the affected cranial nerve, namely the ipsilateral hemitongue in hypoglossal nerve palsy (Figure 8), sternocleidomastoid and trapezius muscles in spinal accessory nerve palsy (Figure 9).

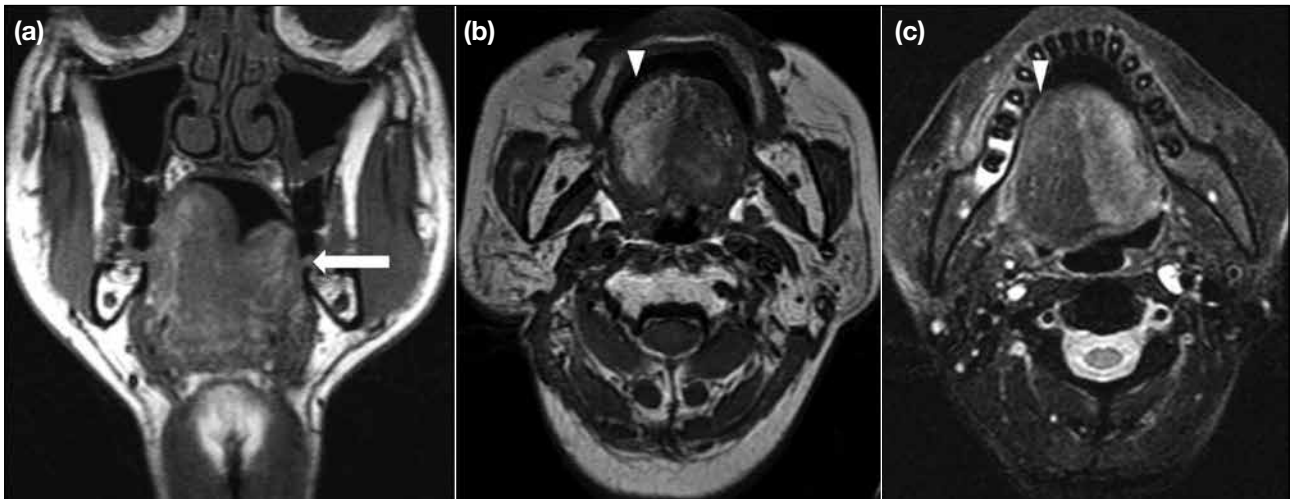


Figure 8. Magnetic resonance imaging in coronal (a) T1-weighted sequence showing atrophy of left hemi tongue (arrow) and axial (b) T1-weighted and (c) T2-weighted sequences showing atrophic right hemi tongue with fatty replacement (arrowheads). These represent chronic denervation from ipsilateral hypoglossal nerve palsy.

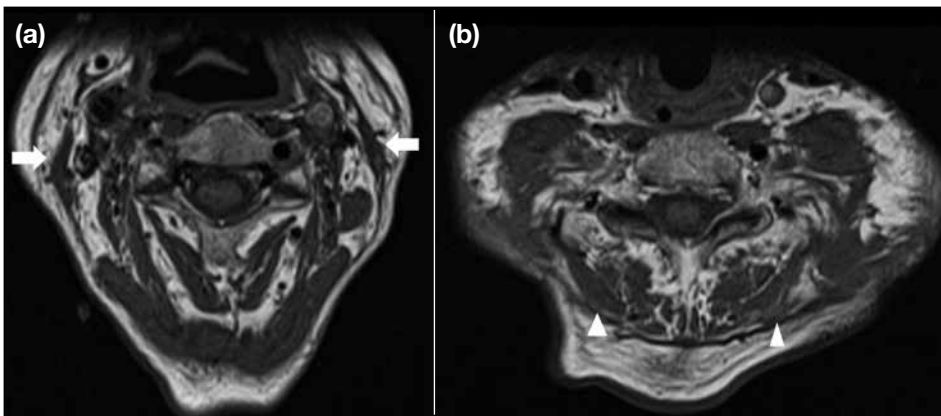


Figure 9. A 51-year-old patient with irradiation for nasopharyngeal carcinoma having spinal accessory nerve palsy with chronic denervation resulting in atrophy of (a) bilateral sternocleidomastoid (arrows) and (b) trapezius muscles (arrowheads).

Brachial Plexopathy

Although injury to the nervous system at the lower neck is less commonly seen nowadays, brachial plexopathy may be encountered occasionally. On MRI, the brachial plexus may appear thickened with T2W hyperintensity and contrast enhancement (Figure 10).¹⁰ Atrophy of the serratus anterior, rotator cuff muscles can be seen in chronic denervation. It has a peak incidence 10 to 20 months post-radiation.

Cerebral Abscess

Cerebral abscess formation may also be encountered, with postulated ascending infection through bony defects from radiation-induced osteitis, sinusitis or mastoiditis.

Irregular rim enhancement can be seen on MRI (Figure 11). It usually demonstrates less restricted diffusion (Figure 12).²

Radiation-induced Osteoradionecrosis

Osteoradionecrosis (ORN) occurs when radiation fibrosis, bony destruction and vascular injury result in tissue breakdown, with the risk highest during the first 6 to 12 months following RT.² These result in bony necrosis and sequestration. Computed tomography detects cortical disruption and loss of marrow trabeculations while MRI shows heterogeneous T1-weighted low-to-intermediate and T2W intermediate-to-high marrow signal (Figure 13). Surrounding soft tissue

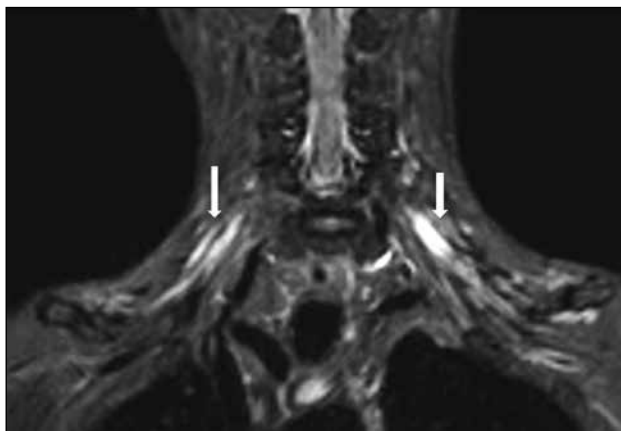


Figure 10. A 61-year-old patient underwent radiotherapy for nasopharyngeal carcinoma and presented with upper limb muscle wasting and numbness. Coronal magnetic resonance imaging short tau inversion recovery (STIR) image showed diffuse fusiform thickening with STIR-hyperintense signal, involving bilateral brachial plexuses, worse on the left (arrows).

mass may be found and can mimic tumour recurrence or superimposed osteomyelitis, rendering radiological diagnosis challenging.² A constellation of clinical findings together with close monitoring and radiological follow-up are helpful and essential in these cases.

Common sites of ORN include skull base and mandible, rarely the cervical spine.¹¹ With disrupted bony cortex of ORN tissue, microbes can ascend to the cranial fossa from paranasal sinuses or the otomastoid system with pneumocephaly. ORN of the mandible can allow spread of dental infections.

For ORN of the mandible, a staging system based on the symptoms, clinical and radiographical findings have been adopted to facilitate patient management. Presence of bony destruction indicates more advanced disease and

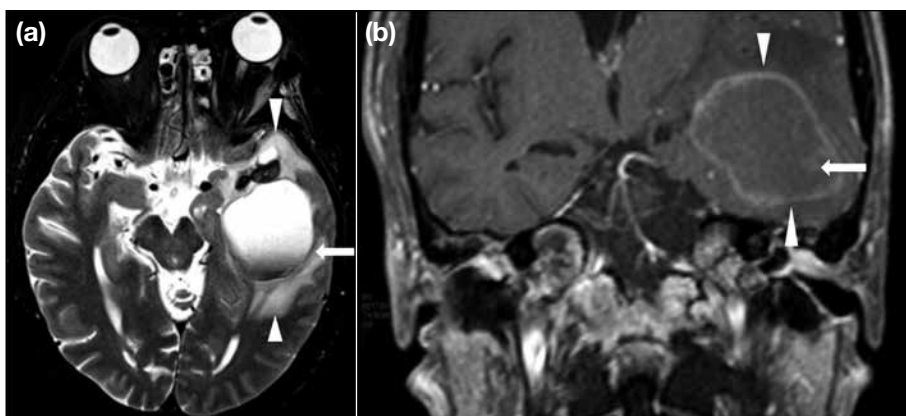


Figure 11. Magnetic resonance images: (a) axial T2-weighted sequence showing a cystic lesion with fluid-fluid level at the left temporal lobe (arrow), with surrounding vasogenic oedema and mass effect (arrowheads); (b) coronal contrast-enhanced T1-weighted fat saturation sequence showing a rim-enhancing lesion at the left temporal lobe (arrowheads) with thin enhancing septum (arrow). Surgical drainage was performed and a specimen grew *Bacillus* species. A prolonged course of antibiotics was prescribed.

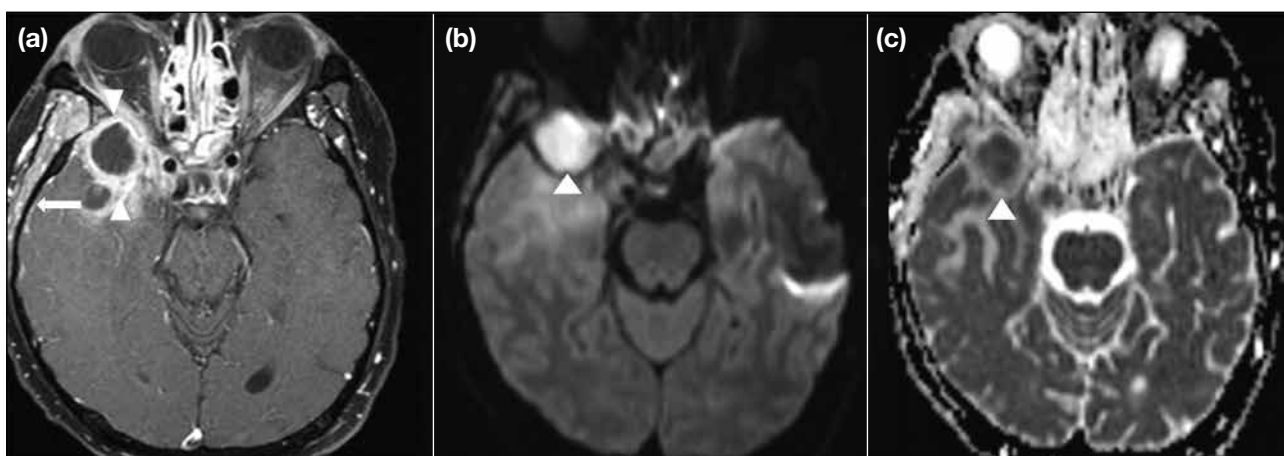


Figure 12. Magnetic resonance images: (a) axial contrast-enhanced T1-weighted fat saturation sequence showing a rim-enhancing cystic lesion at the right temporal lobe (arrowheads) with adjacent leptomeningeal enhancement (arrow), representing cerebral abscess and meningitis; (b) diffusion-weighted image ($b = 1000$) and (c) apparent diffusion coefficient demonstrated restricted diffusion of the right temporal lobe lesion, suggestive of abscess (arrowheads).

need for more aggressive treatment. Dependent on disease stage, treatment ranges from conservative management with antibiotics and mouthwashes to hyperbaric oxygen therapy and ultrasound therapy or surgery.¹²

Radiation-induced Neoplasms

To diagnose a radiation-induced neoplasm, one must occur after a sufficient latency period and histologically differ to the primary tumour.¹ Radiation-induced neoplasm is rare. Common histological types are radiation-induced sarcomas (RIS) and squamous cell carcinomas (SCC).¹³ RIS usually occur 5 to 10 years after radiation, arising in high-dose field zones such as the maxilla and skull base.⁵ Various histological subtypes are observed in RIS, including osteosarcoma and malignant fibrous histiocytoma. Imaging features can be variable but typically include a rapidly growing destructive mass with heterogeneous signals, with or without calcification² (Figures 14 and 15).

SCC typically occur at the temporal bone and external auditory canals and are seen 10 to 15 years after irradiation.³ Like RIS, SCC also carry a poor prognosis¹⁴ and surgery is the only chance of cure, provided the tumour is detected at an early stage.

Radiation-induced Vascular Complications

Accelerated atherosclerosis, thrombosis, and intimal hyperplasia can result in large vessel stenosis and/or occlusion. Imaging findings may reveal atypically located, diffuse and less calcified atherosclerosis.² Atherosclerosis can be found at the common carotid and internal carotid arteries, in addition to the carotid sinus.

Rare but devastating vascular complications include pseudoaneurysm formation, (Figure 16) carotid stenosis or dissection (Figure 17). Therapeutic vascular intervention may be required and includes stenting

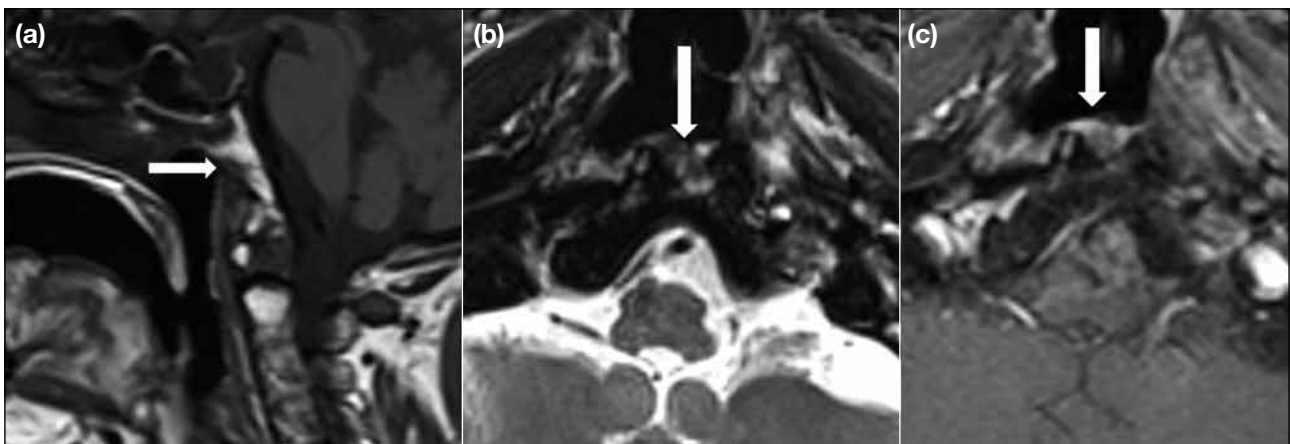


Figure 13. Magnetic resonance images: (a) sagittal T1-weighted, (b) axial T2-weighted, and (c) axial contrast-enhanced T1-weighted fat saturation sequences showing abnormal heterogeneous signal with cortical disruption and enhancement over the anterior aspect of clivus (arrows). The patient remained stable for 3 years with no clinical evidence of recurrence. Features are compatible with osteoradionecrosis.

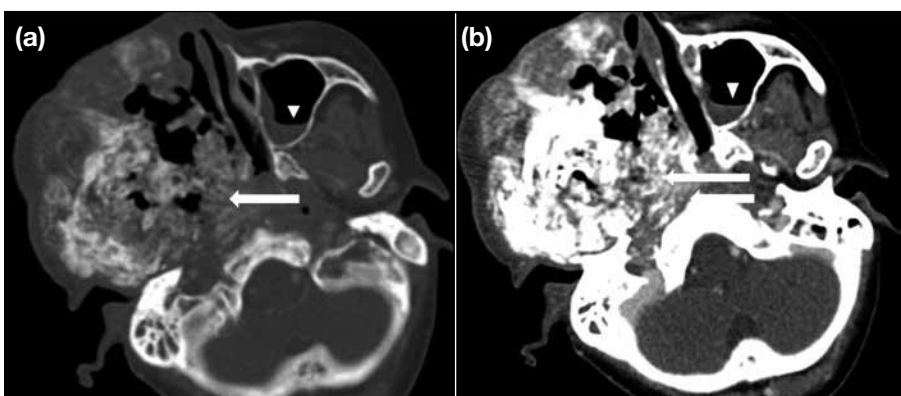


Figure 14. Axial contrast computed tomography scan in (a) bone window and (b) soft window showing an extensive aggressive heterogeneous sclerotic mass with enhancing soft tissue at the right maxilla, histologically proven to be a high-grade sarcoma (arrows). Left maxillary sinus mucosal thickening and right mastoid effusion were also noted (arrowheads).

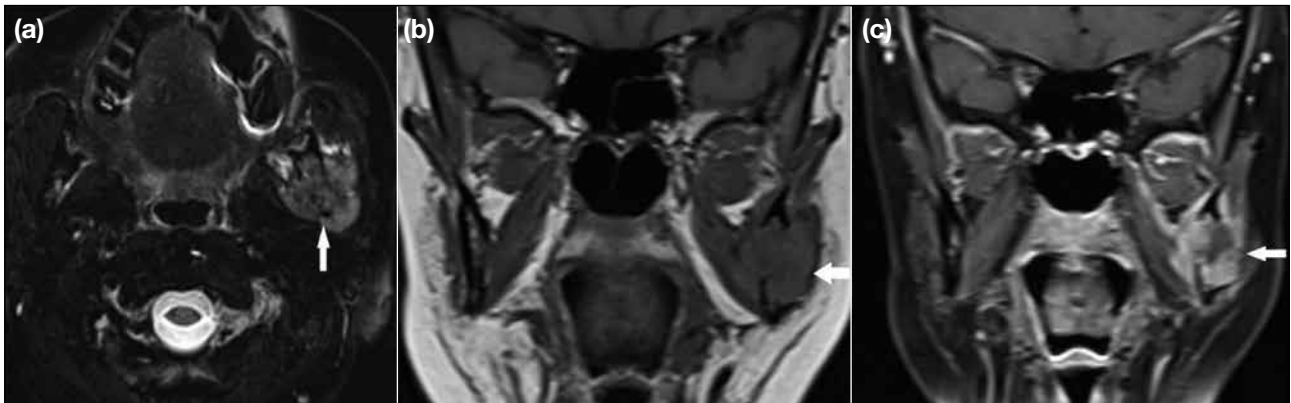


Figure 15. Magnetic resonance images: (a) axial T2-weighted fat saturation; (b) coronal T1-weighted, and (c) coronal contrast-enhanced T1-weighted fat saturation sequences showing a heterogeneously enhancing lesion with bony destruction at the left mandibular body (arrows), with extension to the left medial pterygoid and masseter muscles. This was proven histologically to be a high-grade osteosarcoma.

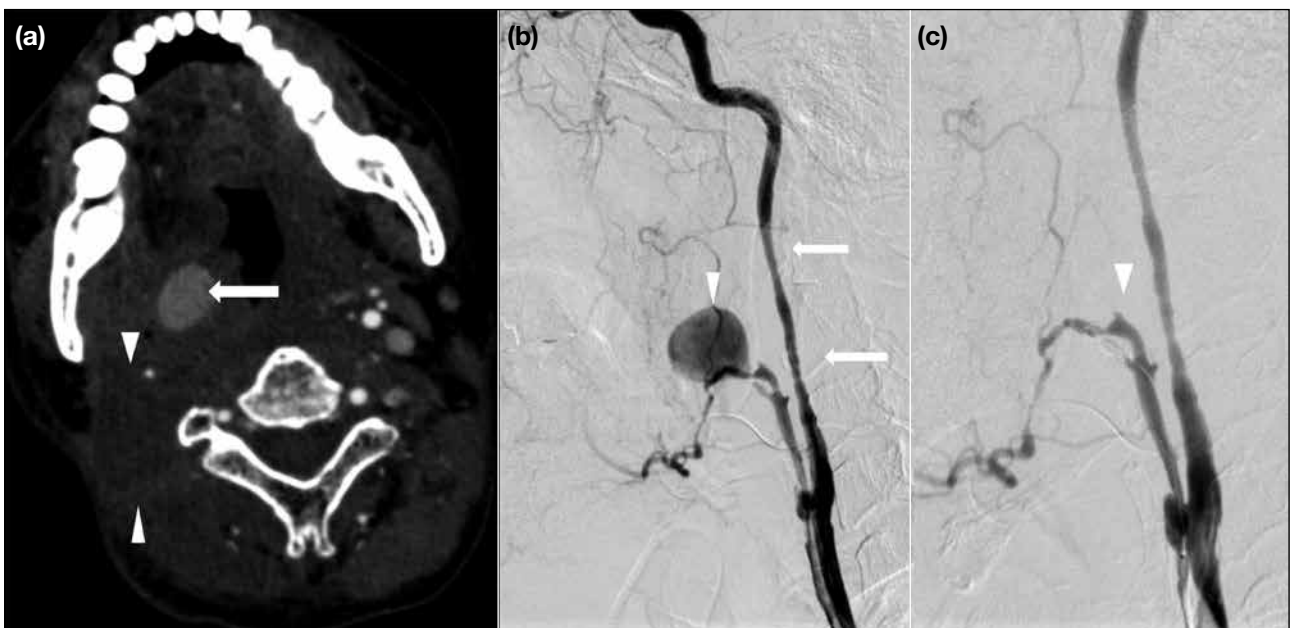


Figure 16. A 51-year-old patient with prior radiotherapy for nasopharyngeal carcinoma presented with breakthrough nose and throat bleeding. (a) Axial computed tomography (CT) angiogram of the neck showed a large pseudoaneurysm arising from the tonsillar branch of the right facial artery (arrow) and a rim-enhancing collection over the right upper neck (arrowheads), which was a seroma shown on prior magnetic resonance imaging; (b) Digital subtraction angiogram (DSA) of the right common carotid artery in lateral view confirms the CT angiogram finding of a large pseudoaneurysm (arrowhead). Long segment irregular stenosis along the included internal and external carotid arteries was also noted (arrows); (c) Post-procedural DSA showing successful coil embolisation (arrowhead).

for stenosis or dissection and coil embolisation for pseudoaneurysm.¹⁵

CONCLUSION

RT, which plays a major role in the treatment of NPC, can cause a wide spectrum of expected post-procedure

changes and complications in the head and neck region. Familiarisation with the relevant imaging features is essential in post-irradiation imaging surveillance to ensure early diagnosis to guide subsequent management. Imaging features atypical of post-irradiation changes should raise the suspicion of other pathologies including



Figure 17. (a) Coronal computed tomography (CT) carotid angiogram showing dissection flap at the right common carotid artery (CCA) [arrowhead]. Long segment severe stenosis over the left common carotid artery was also noted (arrow). (b) Right common carotid digital subtraction angiogram shows irregularity along the right common carotid artery (arrows), compatible with CT angiogram findings. (c) Stenting of the right CCA was performed in the same procedure (arrows).

disease recurrence and radiation-related complications.

REFERENCES

- Bharatha A, Yu E, Symons SP, Bartlett ES. Early and late-term effects of radiotherapy in head and neck imaging. *Can Assoc radiol J.* 2012;63:119-28.
- King AD, Ahuja AT, Yeung DK, Wong JK, Lee YY, Lam WW, et al. Delayed complications of radiotherapy treatment for nasopharyngeal carcinoma: imaging findings. *Clin Radiol.* 2007;62:195-203.
- Glastonbury CM, Parker EE, Hoang JK. The postradiation neck: evaluating response to treatment and recognizing complications. *AJR Am J Roentgenol.* 2010;195:W164-71.
- Yao JJ, Zhou GQ, Xiao LY, Ling LT, Lei C, Yan PM, et al. Incidence of and risk factors for mastoiditis after intensity modulated radiotherapy in nasopharyngeal carcinoma. *PLoS ONE.* 2015;10:e0131284.
- Abdel Razek AA, King A. MRI and CT of nasopharyngeal carcinoma. *AJR Am J Roentgenol.* 2012;198:11-8.
- Chong VF, Fan YF, Mukherji SK. Radiation-induced temporal lobe changes: CT and MR imaging characteristics. *AJR Am J Roentgenol.* 2000;175:431-6.
- Chan YL, Leung SF, King AD, Choi PH, Metreweli C. Late radiation injury to the temporal lobes: morphologic evaluation at MR imaging. *Radiology.* 1999;213:800-7.
- Cheng KM, Chan CM, Fu YT, Ho LC, Cheung FC, Law CK. Acute hemorrhage in late radiation necrosis of the temporal lobe: report of five cases and review of the literature. *J Neurooncol.* 2001;51:143-50.
- Lin YS, Jen YM, Lin JC. Radiation-related cranial nerve palsy in patients with nasopharyngeal carcinoma. *Cancer.* 2002;95:404-9.
- Rehman I, Chokshi FH, Khosa F. MR imaging of the brachial plexus. *Clin Neuroradiol.* 2014;24:207-16.
- King AD, Griffith JF, Abrigo JM, Leung SF, Yau FK, Tse GM, et al. Osteoradionecrosis of the upper cervical spine: MR imaging following radiotherapy for nasopharyngeal carcinoma. *Eur J Radiol.* 2010;73:629-35.
- Chronopoulos A, Zarra T, Ehrenfeld M, Otto S. Osteoradionecrosis of the jaws: definition, epidemiology, staging and clinical and radiological findings. A concise review. *Int Dent J.* 2018;68:22-30.
- Abrigo JM, King AD, Leung SF, Vlantis AC, Wong JK, Tong MC, et al. MRI of radiation-induced tumors of the head and neck in post-radiation nasopharyngeal carcinoma. *Head Neck.* 2009;19:1197.
- Chan JY, To VS, Wong ST, Wei WI. Radiation-induced squamous cell carcinoma of the nasopharynx after radiotherapy for nasopharyngeal carcinoma. *Head Neck.* 2014;36:772-5.
- Lam JW, Chan JY, Lui WM, Ho WK, Lee R, Tsang RK. Management of pseudoaneurysms of the internal carotid artery in postirradiated nasopharyngeal carcinoma patients. *Laryngoscope.* 2014;124:2292-6.